Could biomass-fueled boilers be operated at higher steam temperatures? Part 1: Laboratory evaluation of candidate superheater alloys

DOUGLAS L. SINGBEIL, LAURIE FREDERICK, JAMES R. KEISER, AND W.B.A. (SANDY) SHARP

ABSTRACT: A laboratory-based program was designed to evaluate candidate alloys for superheaters operating at temperatures substantially higher than currently used in practice for biomass and chemical recovery boilers. However, the data is also applicable to superheaters operating in very corrosive conditions at lower temperatures. Alloys are ranked according to their performance in simulated environments.

Application: This paper provides information on the corrosion resistance of alloys that could potentially be used to make superheaters in very advanced biomass and kraft recovery boilers with superheater steam temperatures much greater than 500°C. Nearly all the alloys would be effective at preventing corrosion of superheater tubes that operate in more normal conditions for existing boilers.

Biomass is increasingly looked on as a cost-effective, environmentally friendly alternative to coal and petroleum-based fuels in the generation of energy. However, relative to coal and fuel oils, biomass-based fuels are inhomogeneous, and they also contain significant impurities, such as chlorides, alkali metals and heavy metals, that deposit on heat transfer surfaces. While these deposits may reduce the overall energy efficiency of the boiler, their principal effect is to cause rapid corrosion of heat transfer surfaces that approach, or exceed, the first melting point of the deposits. As a consequence, boilers burning biomass have largely been limited to operating with superheater steam temperatures of less than 510°C (950°F) and steam pressures of less than 11 MPa (1600 psi). The bulk of existing biomass boilers in North America operate at substantially lower steam temperatures and pressures, particularly those utilized as waste utility boilers and kraft recovery boilers. In contrast, the most modern utility boilers burning coal are intended to operate at 26 MPa (3800 psi) with 615°C (1140°F) superheated steam temperatures, and research programs are in-place to help design and build even more efficient boilers by the year 2015.

While small, incremental gains in energy efficiency can be met by improving operation of existing biomass-fired boilers, the greatest overall gain comes from designing and building biomass boilers that operate at substantially higher pressures and superheater steam temperatures (HT/HP) than is the current practice. To gain this enhanced energy efficiency and retain operational reliability, challenging materials problems in the areas of high temperature strength and environmental degradation must be overcome, particularly at temperatures near or above the first melting point of the superheater tube deposits. These issues were addressed in a multi-year research program that comprised several tasks to explore and expand the operating envelope of future biomass-fueled steam generating systems. The program's tasks included a literature review [1]; an assessment of European best efforts to circumvent such problems [2]; an economic assessment of the value of operating boilers with more aggressive superheater steam temperatures and pressures [3]; and laboratory studies in simulated service environments, and *in situ* deposit and corrosion probes [4,5]. Further background about the program and discussion of issues related to corrosion of superheater tube materials can be found in detail in these earlier references, and will not be repeated here. Results from the laboratory studies in simulated service conditions in kraft recovery and biomass-fired boilers are presented in this paper.

EXPERIMENTAL PROCEDURE

Overview

A test matrix was developed to evaluate materials in simulated superheater deposit environments based on the analysis of deposits from the three operating boilers used in the program – one recovery boiler and two biomass-fired boilers. A total of 25 tests were completed over the course of the program, ranging in length from 100 to 1000 h (**Table I**). Complete experimental details can be obtained from the final program report [6]; what follows is a brief synopsis of the important details.

		Simulated Deposits				
	Hours	RB			PB1	PB2
		510°C	530°C	625°C	650°C	650°C
Alloy Set 1	100	T1	-	T5	T9	T13
	200	T2	-	T6	T10	T14
	500	T3	-	T7	T11	T15
	1000	T4	T17	T8	T12	T16
Alloy Set 2	1000	T20	T24	T21	T22	T23
Alloy Set 3	1000	T27*	T28*	T29*		

* Cover gas for these tests included 50 ppm SO_2.

I. The test matrix for the laboratory program. Cover gas for all experiments contained 5% O_2, 10% CO_2, 20% H_2O, balance N_2. Makeup of alloy sets is shown in Table II.

Test temperatures

The principle established for selecting the test temperatures was to set a target for metal temperature of 100°C higher than the current maximum operating superheated steam temperature for the type of boiler. This was anticipated to provide a challenging, but realistic, stretch target for alloys and new boiler design. Since tube surface temperatures are higher than the steam temperature in service, this implies less than 100°C increase in steam temperature.

In the case of the recovery boiler, very few boilers worldwide operate with superheater steam temperatures of 525°C, and so the maximum test temperature was chosen to be 625°C. Additional tests were conducted at 510°C – a temperature below the first melting temperature (FMT) of the synthetic deposit, and 530 °C – just above the FMT of the deposit. Some European wood-fired boilers operate with 550°C superheated steam [1,2], so the maximum test temperature for those tests was chosen to be 650°C. The FMT for the bark-fired power boiler deposits was greater than 700°C. This is a much higher temperature than the boilers could reasonably be expected to operate, even during upset conditions. Consequently, no tests were carried out at the FMT of the biomass boiler deposits.

Deposit chemistry

The synthetic salts used for the bark-fired boiler tests were based on analyses of deposits from air-cooled probes installed in the model biomass-fired boilers [4]. One was considered to be very aggressive, with high levels of chloride and potassium, while the other was representative of a much cleaner fuel. The recovery boiler salt composition was tailored to provide a salt with an FMT of 525°C. It is the same as that used in previous work by FPInnovations and was based on analyses of superheater deposits in several boilers, including the recovery boiler from the pulp mill used as the host for the long-term corrosion probe work [4]. **Figure 1** shows the composition of the simulated deposits as an elemental mole fraction. Batches of the salts were made in bulk using ACS reagent grade salts

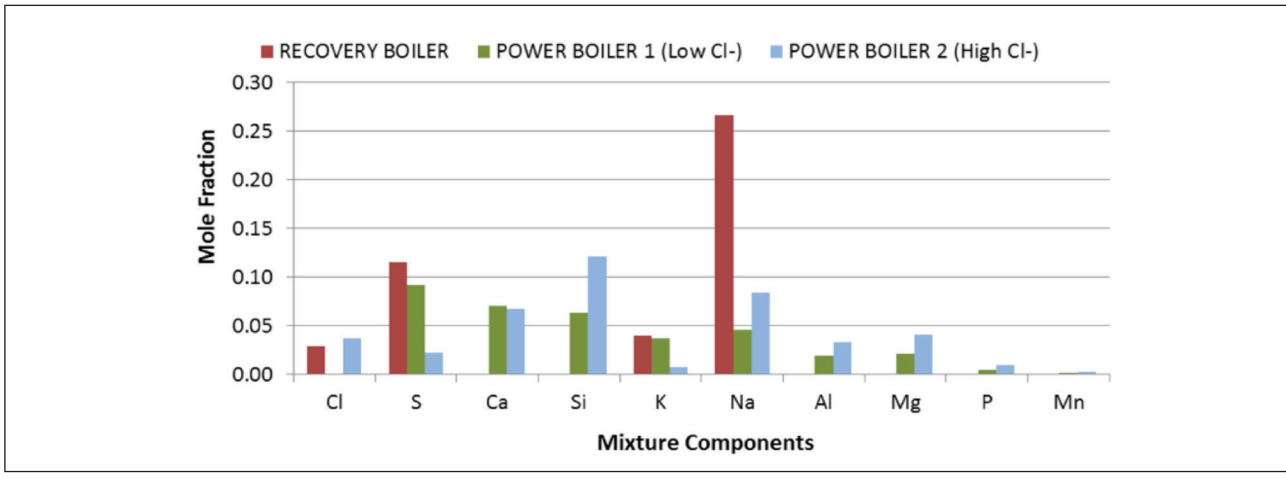

1. Graphic representation of the three salt compositions used in this work.

Code	UNS No.	Alloy Set 1	Alloy Set 2	Alloy Set 3
A	S21500	X		X
B	S31009	X	X	X
C	N08028	X		
D	N08120	X	X	X
E	N06025	X		X
EP	N06025 pre-oxidized	X	X	
F	N07214	X		
FP	N07214 pre-oxidized	X		
G	R20033		X	
H	S33228		X	X
I	N12160		X	X
J	N06059		X	
K	N06690		X	X

II. Alloys used in each alloy set. Due to limited space for data in tables and graphs, codes are used throughout the report to represent the alloys.

when available. The mixtures of compounds were placed into a porcelain milling jar and tumbled with high purity alumina balls for 45-60 min. The resultant powder was passed through a 100 mesh screen and the FMT checked by differential thermal analysis (DTA) before being accepted for use.

Cover gas composition

The gas mixture used for all but three tests was 5 vol% oxygen (O_2), 10 vol% carbon dioxide (CO_2), and 20 vol% water (H_2O). The balance was N_2. A small amount of sulfur dioxide (SO_2), 50 ppm, was added to the cover gas for the final three tests. The flow of each gas, except for water vapor, was controlled by a mass flow controller (MFC). The total of 200 standard cm^3 produced a linear flow rate of 5 cm/min through the furnace tube. The accuracy of the controllers was ±3-5% of the setpoint, depending on the gas and capacity of the MFC. The flow of distilled water was controlled by a precision peristaltic pump, and the water was added directly into the gas inlet end of the furnace tubes. Tests showed that the water vaporized before reaching the tube wall. The water flow varied as the pump tubes aged and had to be monitored daily and adjusted on occasion. Analysis of the daily water usage data showed the volume % H_2O normally ranged between ±5 vol% of the setpoint.

Alloys

The choice of alloys was based on consultations with boiler owners, manufacturers, and alloy suppliers participating in this project as industrial partners, as well as consideration of the literature and experience with these alloys in other types of service. Not all of these alloys are currently available as code-certified tube material; the first premise was to choose alloys for their anticipated corrosion resistance in the test environments. The alloys are listed in **Table II** by Alloy Set, where each set is the

CODE	Product Name	UNS No.	Fe	Ni	Cr	Mo	Co	Al	Mn	Si	Ti	C	Others
A	Esshete 1250*	S21500	67	10	15	1			6.3	0.2 - 1.2			V=0.15-0.4
B	31OH	S31009	Bal	19.4	24.3	0.088	0.2	0.028	1.57	0.41	<0.01	0.059	Cu=0.09
C	Sanicro 28	N08028	Bal	30.4	26.7	3.33			1.74	0.43		0.01	Cu=1.06, N=0.081
D	HR120	N08120	Bal	37.3	24.92	0.26	0.15	0.07	0.72	0.45	<0.01	0.044	Nb=0.61, N=0.22, Cu=0.07, B=0.002
E	602CA**	N06025	9.6	62.2	25.3			2.3	0.02	0.03	0.1	0.17	P=0.05, Z=0.09, Y=0.07
F	HR214**	N07214	3.86	~75	16.1	<0.1	0.01	4.34	0.21	0.06	<0.001	0.01	B=0.002, Zr=0.011, Y=0.004
G	A33	R20033	32.4	30.85	33	1.49			0.61	0.24		0.015	Cu=0.61, N=0.43
H	AC66	S33228	Bal	31.8	27.09			0.01	0.5	0.21		0.06	Nb=0.8, Ce=0.08
I	HR160	N12160	0.63	~37	28	0.27	30.2		0.48	2.75	0.48	0.056	
J	A59	N06059	0.6	60.19	22.9	15.5	0.1	0.3	0.17	0.02		0.004	Cu=0.01
K	A690	N06690	8.7	62.5	27.85				0.2	0.15		0.02	Cu=0.01

* Nominal values. ** Alumina former.

III. Nominal compositions of alloys evaluated in the test program.

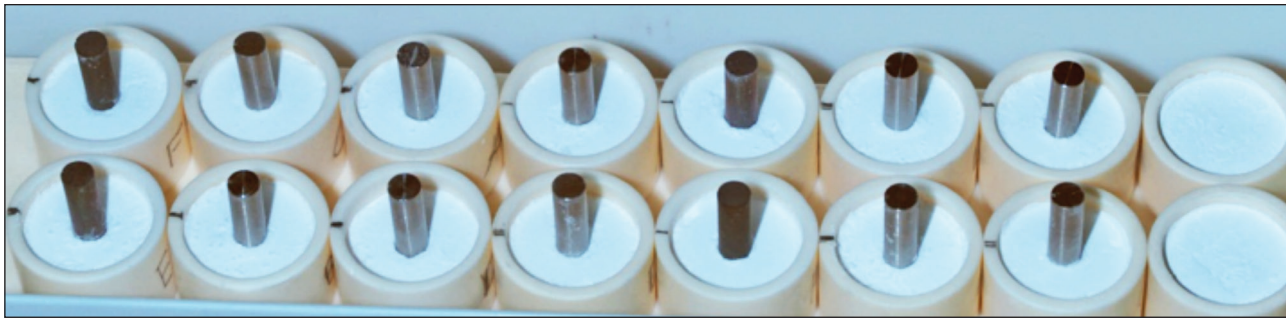

2. Alloy Set 1 laid out in preparation for insertion to a furnace, showing the reproducibility of the initial salt packing and surface height. The pre-oxidized coupons in the third and last rows from the right are darker than the remaining as ground coupons. Blank "guard" pots placed at the gas inlet are also visible.

alloys exposed together in a single furnace test. Nominal composition of the alloys is shown in **Table III**, along with the single letter code adopted for use in all documentation. The baseline alloy for both laboratory and *in situ* field tests was S31009, although the field trials also included S347009, which is a commonly used comparable alloy in North America [4].

Peg coupons were produced from each alloy with dimensions 25 mm long x 5 mm dia., with a 0.4 to 1.6 µm Ra ground finish. A notch was cut in one or both ends of each peg coupon to act as an indicator of coupon orientation relative to the direction of gas flow in the furnace. The coupons were cleaned and dried with blowing hot air. The diameter of each peg coupon was measured with a micrometer (+2.5 µm) at three points around either end and in the middle of the cylinder. These measurements were averaged for each location and used as the "before exposure" diameters during post exposure analysis. The peg coupons were cleaned and stored in plastic containers until use.

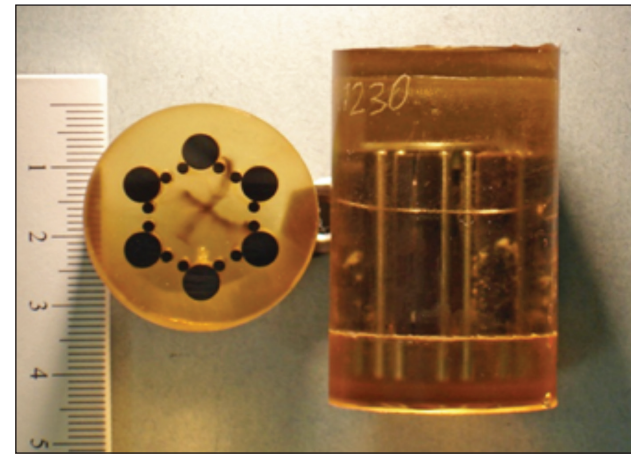

3. Six coupons embedded in epoxy with their support pins. The mount on the right has not been machined square yet. The mount on the left has been dry sectioned.

Exposures

Peg coupons were placed in alumina crucibles and synthetic salts packed around the circumference (**Fig. 2**). The pegs were taller than the crucibles, and hence permitted exposure of each specimen to both the gas phase within the furnace (including corrosive vapors) and to coverage by a bed of synthetic salt. Fourteen crucibles at a time (with at least two of each alloy) were placed onto an alumina "D" support platform, and placed in the center of a horizontal tube furnace. Coupon orientation on the "D" support platform was noted and remained consistent from test to test. More alloys were evaluated than space allowed in a single test, so in some cases, sets of coupons were independently exposed to the same test conditions. Once the coupons were sealed in the furnace under flowing nitrogen, the temperature was ramped slowly to the set point. When it was reached, the test gases and water were introduced into the furnace. At the conclusion, the coupons were allowed to cool in the furnace with flowing nitrogen as a cover gas.

Analysis

Coupons were photographed immediately on removal from the furnace, and then carefully pried from the crucible with the salt layer as intact as possible. Six coupons at a time were fitted to a jig, and embedded in an epoxy metallographic mount for sectioning and cross-sectional polishing (**Fig. 3**). Each mount was sectioned at a point above and below the level of the salts in the crucible. Sections were then dry-polished to a 3 µm diamond finish and the surface of each coupon photographed using a 10X objective in an automated Zeiss AxioVision microscope (Carl Zeiss Microscopy; Jena, Germany) to create a mosaic image. In total, more than 350 coupons were exposed in the test program, leaving some 700 surfaces to analyze. For coupons with more than 25 µm of corrosion, a custom image analysis program was developed, employing Otsu's Method and a circle fitting function to determine the original coupon center prior to segmenting the coupon into 24 arcs. Measurements were made for both the maximum metal loss and total-affected-metal (TAM) in each arc (**Fig. 4**). Metal loss was determined at the interface between the scale and sound metal, while the TAM for the coupon was defined as the average of the deepest visible penetration of corrosion into the interior of the coupon in each of the 24 arcs. The accuracy of the measurement was estimated to be ±3 µm.

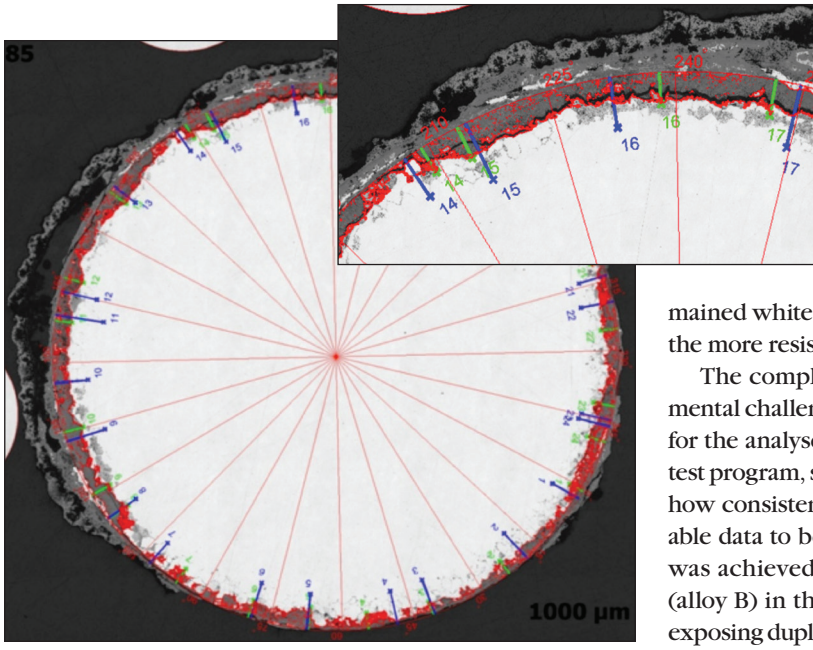

4. A mosaic image of a cross-section after analysis. Inset shows top right corner in more detail. The outer red circle is the original circumference of the coupon. The green lines indicate the depth measured for metal loss, and the blue lines indicate the total affected metal measurement for each of the 24 arcs around the circumference. The average of the 24 total affected metal measurements is defined as the TAM of the coupon.

RESULTS AND DISCUSSION

Overview

An example of the general appearance of the coupons after exposure is shown in **Fig. 5**. These coupons were exposed to the recovery boiler salts at 625°C. Yellowing at the surface of the salts was observed in many tests, but to a far greater extent in the recovery boiler salts. EDX analysis of yellow and white salts confirmed that the yellow color was associated with chromium. Sodium chromate (Na_2CrO_4) is an intense yellow salt that appears the most likely to have been formed. On several occasions, and for more than one alloy, it was noted that when one of a pair of coupons within a given test had corroded significantly more than the other, the salts had remained white for the corroded coupon and had yellowed for the more resistant.

The complex test environment presented many experimental challenges, both in the setup and operation, as well as for the analyses of the coupons afterwards. Throughout the test program, steps and checks were put in place to determine how consistent conditions were from test to test, and to enable data to be compared and normalized across tests. This was achieved by putting two baseline coupons of S31009 (alloy B) in the same locations of the furnace in every test, exposing duplicate coupons of every alloy, and exposing some alloys (S31009, N06025, S21500) in all three alloy sets.

It is clear from an examination of the data that conditions within the furnaces were not always identical, and neither were conditions in duplicate tests. Nonetheless, the data proved to be reasonably consistent within, as well as between, tests. A few tests produced highly variable data that was almost certainly caused by artifacts in the test environment. The stochastic nature of corrosion was also demonstrated as greater variability was found in the shorter-term tests due to the randomness of initiation events on the coupons. Results in the longer-term tests were more uniform.

A total of fifty S31009 (alloy B) coupons were exposed over the entire program, giving 100 sections to be analyzed (half in the vapor phase and half under-deposit). Data was analyzed from the 50 individual S31009 sections for which the TAM was greater than 25 µm. The standard deviation of the 24 TAM measurements around the circumference as a percent of their

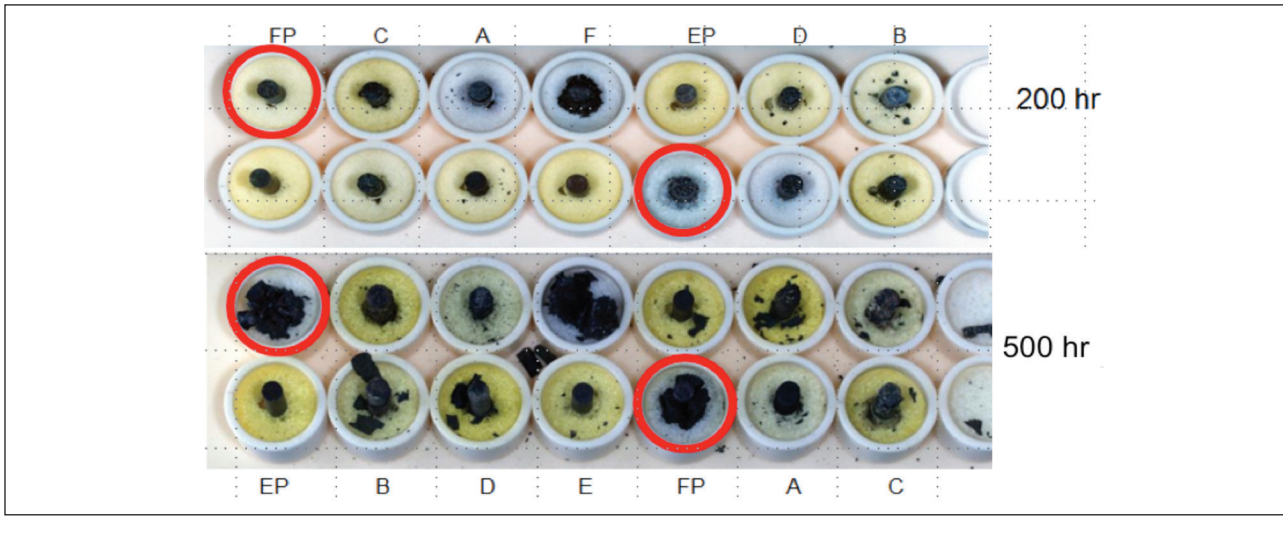

5. Appearance of coupons at the conclusion of tests in RB salts at 625°C. Red circles indicate coupons of pre-oxidized HR214 (Alloy FP). Note that the only Alloy FP coupon not to show substantial spalling is the one with the yellow-shaded salt.

		Standard Deviation as % of Average TAM		
Code	**Alloy**	**Vapor Phase**	**Under-Deposit**	**Average**
H	S33228	14%	17%	16%
B	S31009	18%	14%	16%
C	N08028	18%	20%	19%
A	S21500	24%	20%	22%
J	N06059	-	22%	22%
D	N08120	24%	24%	24%
K	N06690	26%	23%	25%
EP	N06025 pre-oxidized	24%	26%	25%
E	N06025	34%	32%	32%
F	N07214	38%	28%	33%
FP	N07214 pre-oxidized	42%	29%	33%
I	N12160	29%	38%	34%
	Average Standard Deviation %	26%	24%	

IV. Standard deviation in average TAM for alloys for all the test environments. The data is separated into vapor phase and under-deposit results and sorted by the average of those results.

average was calculated for each coupon. It ranged from 7% to 62% above the salts with an average of 15%, and from 5% to 30% below the salts with an average of 18%. The overall average of the above for S31009 is 16%. For the balance of the alloys, the standard deviation for any given set of measurements in duplicate tests fell between 15% and 25% of the average TAM for the alloy, consistent with the S31009 result. Only three materials fell outside of this range – those with the most severe corrosion and those with the least corrosion (**Table IV**).

Power boiler 1 (PB1) tests

The PB1 salt was representative of deposits produced by clean, uncontaminated fuel. There was minimal corrosion on all coupons exposed to this salt, even for tests that lasted 1000 h. The average TAM was far less than 25 µm for all coupons.

Power boiler 2 (PB2) tests

The PB2 salt was representative of deposits produced by fuel that is highly contaminated with chloride. Even so, the depths of corrosive attack on all coupons were much less than 25 µm after 100 h. Only coupons from test exposures 200 h and longer were subjected to the full standard analysis. Corrosion as a function of time is shown in **Fig. 6**, while results for the 1000-h tests are shown in **Fig. 7**, plotted in order of increasing nickel content in the alloys. The most extensive corrosion in these tests occurred underneath the layer of salt; there was

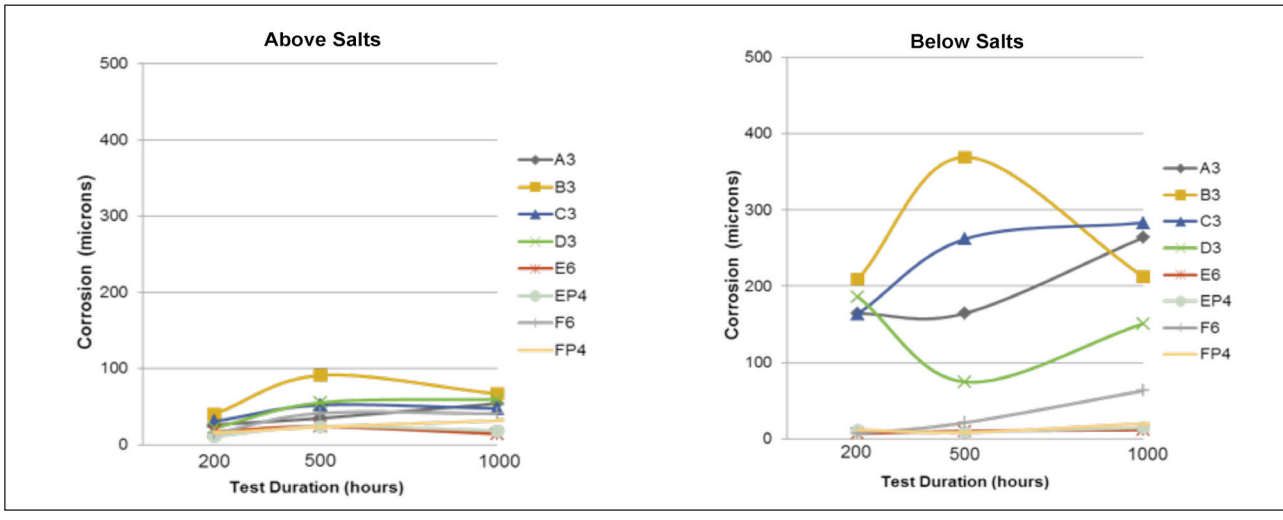

6. Variation of average TAM with time in PB2 salts at 650°C (T14, T15, T16), in µm.

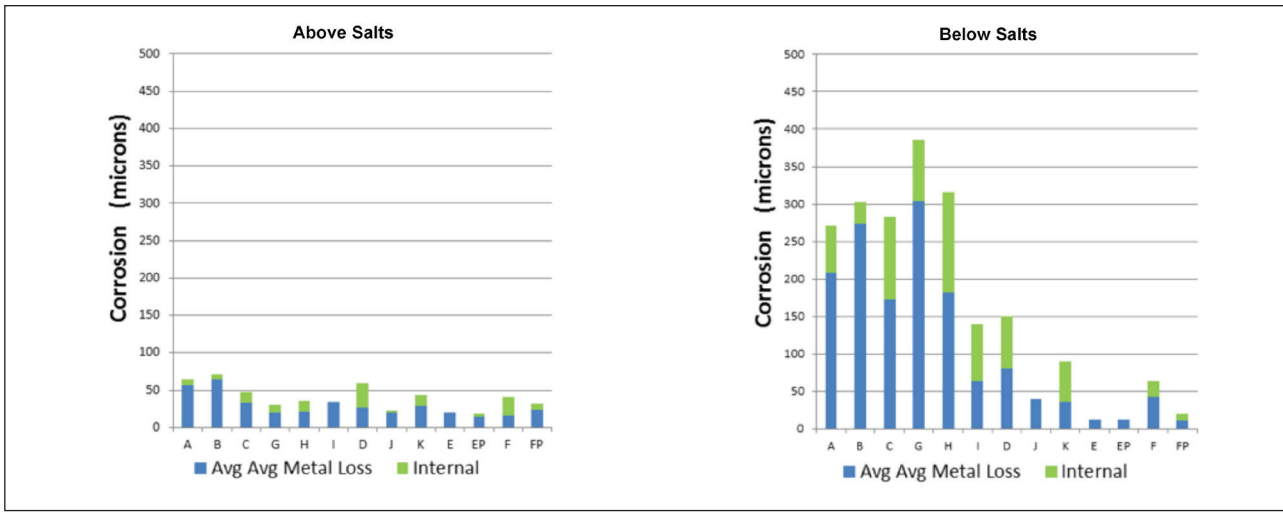

7. Test data from alloys exposed to PB2 salts for 1000 h at 650°C. Alloys are listed in order of increasing nickel content left to right, with the last four on the right being the alumina formers (E, EP, F, FP). Metal loss is blue portion of bar, TAM is green portion of bar.

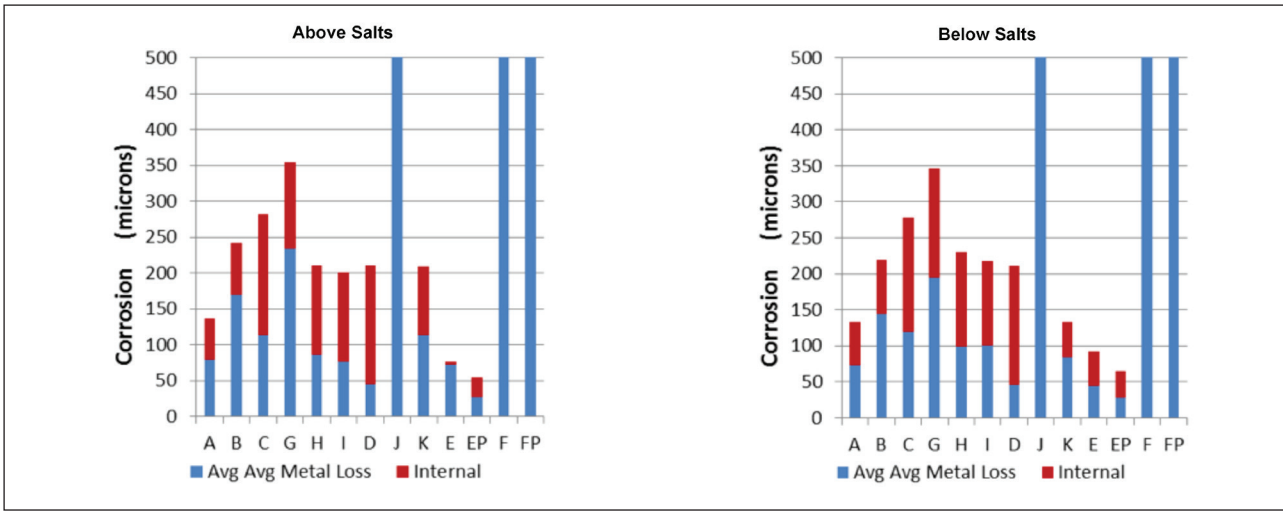

8. Test data from alloys exposed to RB salts for 1000 h at 625°C. Metal loss is blue portion of bar, TAM is red portion of bar. The alloys are listed in order of increasing nickel content, left to right, with the alumina formers at the right (E, EP, F, FP).

much less corrosion above the salt layer. There is also a clear correlation between increased resistance to corrosion and greater nickel content of the alloy. Conversely, there was no correlation when the same data was plotted as a function of chromium content. The results from the test conducted for 500 h appear anomalous and a review of the data showed higher than average variation in TAM on several coupons. No reason for this variation was discovered.

Recovery boiler tests

Negligible corrosion was observed on the alloys in tests conducted at 510°C; the greatest TAM measured was only 17 µm for N06025 (alloy E). This temperature is below the FMT of the salt deposits. More substantial corrosion was observed at both higher temperatures, and two alloys completely disintegrated in the 1000 h test at 625°C. These were N07214 (alloy F) and N06059 (alloy I). Data for the 1000 h tests at 625°C is shown in **Fig. 8**. The correlation between corrosion and nickel content is not apparent in these tests; nor does the corrosion correlate with chromium content of the alloys. Of significance in these tests was the observation that corrosion in the gas phase was nearly as severe as underneath the salt deposits. Especially in the vapor phase, internal penetration accounted for a larger proportion of the TAM. A measureable increase in corrosion was noted for many of the alloys when SO_2 was added to the cover gas (**Fig. 9** and **Fig. 10**).

Alloy performance and ranking

Evaluation of alloy performance was based on the results of 1000 h tests, and compared the average TAM from all coupons of the same alloy in each environment, as well as visual and microscopic observation of the coupons. An arbitrary scale was used to rank the alloys. An average TAM of less than 25 µm was considered acceptable, between 25 and 50 µm was

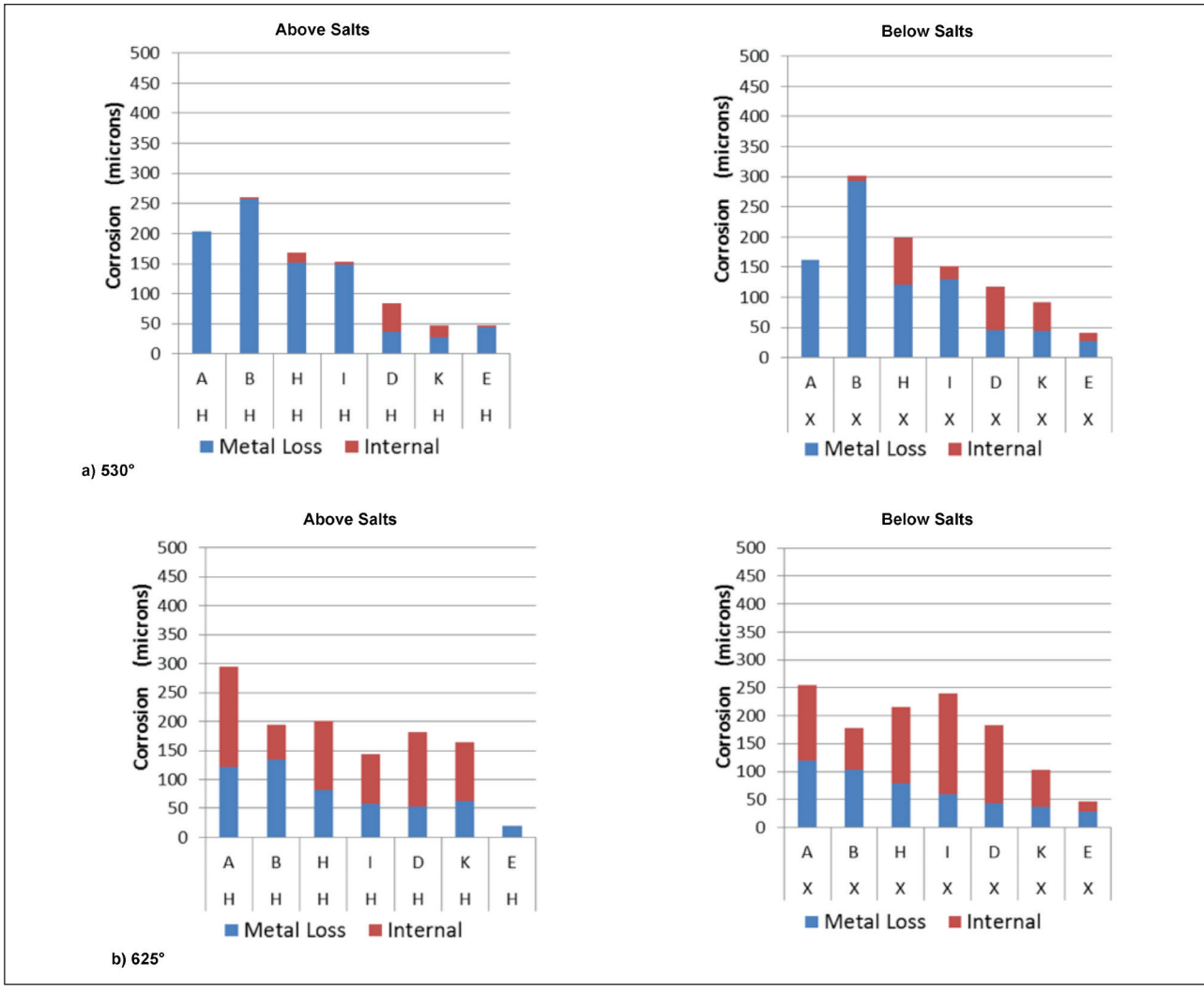

9. Corrosion results for Alloy Set 3 after exposure to recovery boiler salts at (a) 530°C and (b) 625°C for 1000 h in the standard atmosphere plus 50 ppm SO_2.

intermediate, and greater than 50 µm was considered unacceptable performance. For reference, linear corrosion at 25 µm/1000 h would extrapolate to 2.2 mm over 10 years and 50 µm/1000 h would represent a loss of nearly 4.4 mm over a 10 year life. The ranking of alloys was different for each environment, and also varied by temperature in the same environment.

In the PB1 environment at 650°C, all alloys performed well enough to fit into the acceptable category.

In the PB2 environment at 650 °C, only three alloys fell into the acceptable performance range above the salt deposits (**Fig. 11**). A number of other alloys performed moderately well in the vapor space above the salts, but did much more poorly underneath the deposits. The best three alloys overall in the PB2 salts were N06025 (alloy E), N06059 (alloy J), and the pre-oxidized N07214 (alloy FP). As already mentioned, there was a general correlation between increasing nickel content in the alloy and better performance in this environment. This correlation was less apparent in the vapor space than beneath the salts. Two of the alloys that performed moderately well in the vapor space were R20033 (alloy G) and S33228 (alloy H). These two alloys are among the group of four alloys with the lowest nickel content, and did very poorly beneath the salts. The other low nickel alloys were S31009 (alloy B) and S21500 (alloy A), both of which fared quite poorly above and below the salt deposit in these tests.

In the recovery boiler environment at 510°C, all alloys provided acceptable corrosion resistance. At 530°C, the only alloy to provide acceptable service both above and below the salt level was N06059 (alloy J) (**Fig. 12**). A few other alloys – notably N06025 (alloy E & EP) and N07214 (alloy F) – were acceptable in the vapor space, but not beneath the salts. N06690 (alloy K) and N12160 (alloy I) fell into the intermediate category above the salts, and N06025 (alloy E) was the only alloy to fit into the intermediate category beneath the salts. The worst alloys in this service were S31009 (alloy B), S21500 (alloy A) and S33228 (alloy H).

As expected, the recovery boiler environment at 625°C was

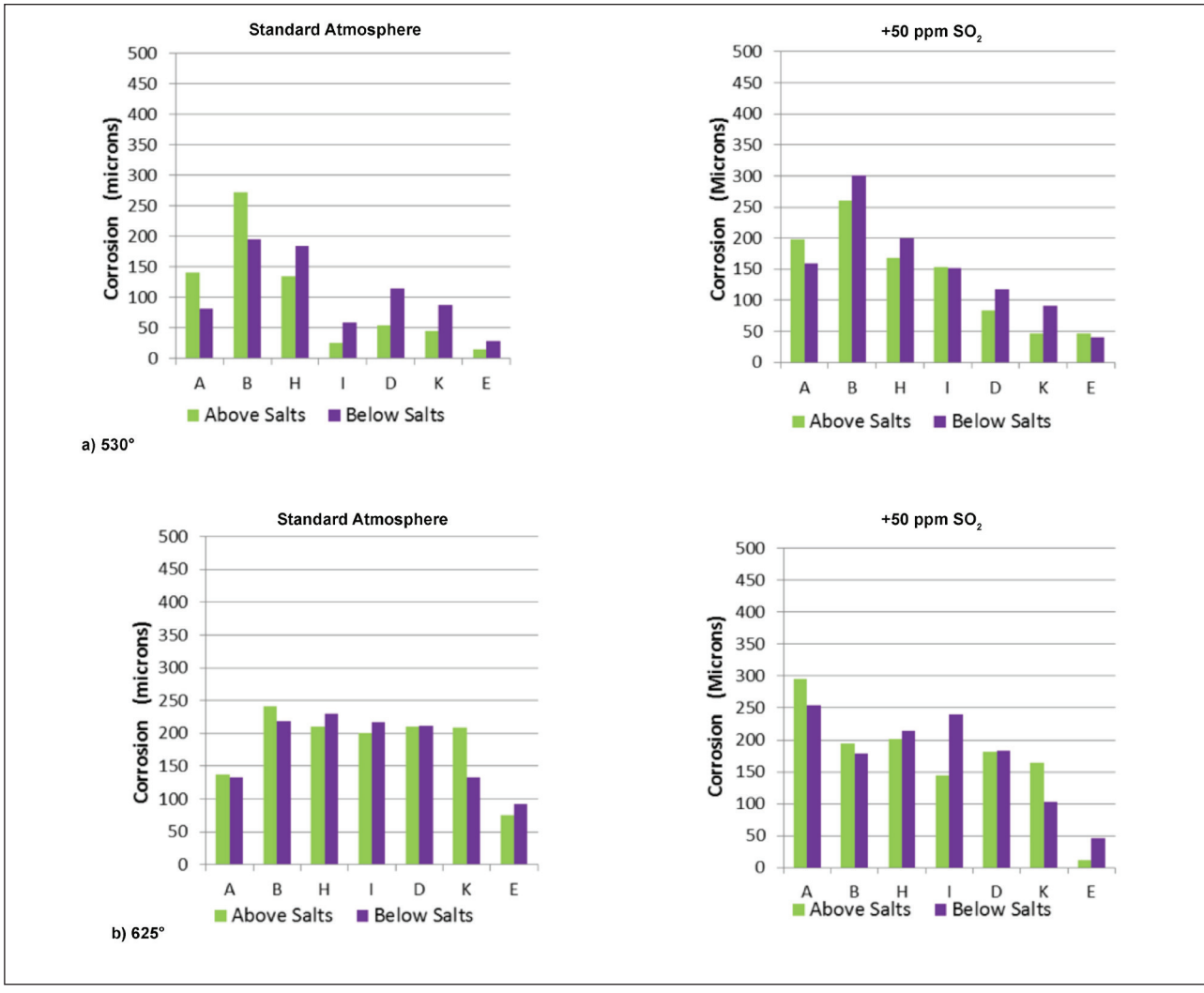

10. Comparison of average TAM for the alloys that were in recovery boiler 1000 h tests, without and with the addition of 50 ppm SO_2. (a) 530°C; (b) 625°C.

Section	PB2 650°C												
Above salts	E	EP	J	G	FP	I	H	F	K	C	D	A	B
	18	18	23	31	31	35	36	41	44	47	59	65	71
Below salts	E	EP	FP	J	F	K	D	I	A	C	B	H	G
	10	12	20	38	63	89	151	154	271	283	303	316	385

TAM (μm)/1000hr	
10	< 25
30	≥ 25 < 50
271	≥ 50

11. The average TAM in microns for each alloy exposed to the PB2 environment at 650°C. Alloy performance is color coded as acceptable (green), intermediate (yellow), and unacceptable (red).

extremely aggressive and no alloy fit into either the acceptable or intermediate categories (**Fig. 13**). Corrosion rates above and below the salt level were similar. N06025 (alloy E) was the best of the alloys, along with S21500 (alloy A) and N06690 (alloy K). Two alloys failed catastrophically in the recovery boiler environment at 625°C – N06059 (alloy J) and N07214 (alloy F). The failure of N06059 (alloy J) was unexpected, given its extremely good performance in the same environment at the lower temperature. This alloy stands out from the others due to the very high molybdenum content, and it is possible that this is a contributing factor to the failure at the higher temperature. A boundary between hexagonal MoS2 and monoclinic Mo2S3 exists at 664 ± 50°C [7], but whether such a change could contribute to a dramatic increase in corrosion is unknown. N07214 (alloy F), in contrast, contains little molybdenum, but contains the second least amount of chromium (next to S21500 [alloy A]). Chromium is well known to enhance corrosion resistance in kraft recovery environments, so

Section	RB 530°C													RB 530°C +SO_2						
Above salts	J	F	E	EP	I	FP	K	D	G	C	H	A	B	K	E	D	I	H	A	B
	12	13	15	15	25	42	44	54	62	127	133	140	272	47	47	83	154	168	198	260
Below salts	J	E	EP	I	F	A	K	G	D	FP	C	H	B	E	K	D	I	A	H	B
	14	27	39	59	61	81	87	99	115	159	169	185	194	41	91	118	151	160	199	301

TAM (µm)/1000hr	
10	< 25
30	≥ 25 < 50
271	≥ 50

12. The average TAM in microns for each alloy exposed to the recovery boiler environment at 530°C. Alloy performance is color coded as acceptable (green), intermediate (yellow), and unacceptable (red).

Section	RB 625°C													RB 625°C +SO_2						
Above salts	EP	E	A	I	K	D	H	B	C	G	J	F	FP	E	I	K	D	B	H	A
	55	76	137	201	209	210	211	242	282	355	2000	2000	2000	12	144	165	182	195	201	295
Below salts	EP	E	K	A	D	I	B	H	C	G	J	F	FP	E	I	K	D	B	H	A
	65	92	133	134	211	217	219	230	278	347	2000	2000	2000	46	103	179	184	215	241	255

TAM (µm)/1000hr	
10	< 25
30	≥ 25 < 50
271	≥ 50

13. The average TAM in microns for each alloy exposed to the recovery boiler environment at 625°C. Alloy performance is color coded as acceptable (green), intermediate (yellow), and unacceptable (red).

the failure of N07214 (F) was not unexpected. In contrast, the relatively good performance of the S21500 (alloy A) coupons in this environment was surprising, given the low chromium content of this alloy. While it might be argued that the manganese content of this alloy imparted some level of protection, there remains the possibility that it too might have failed catastrophically had the test been prolonged.

The ranking of alloys in the SO_2-containing cover gas were similar to the equivalent results in tests without SO_2. Only 7 of the alloys were exposed in this environment, and they were chosen as the best of the previous tests. 602CA (alloy E) displayed by far the best corrosion resistance in this test. There appeared to be little difference in corrosion above or below the salt level. S21500 (alloy A) and S31009 (alloy B) were the worst of the limited set of alloys exposed to the SO_2-containing environment. Given that the standard deviation of these experiments varies between 15%-25%, the performance of the balance of the other alloys could be described as similar.

Comparison to field data

Laboratory experiments are typically well-controlled and provide more reproducible results than field exposures, where temperature, deposit flux and composition, and other critical parameters vary dramatically as a function of time. The intent of laboratory experiments is to provide comparable data in less time, with useful results. Often, they also fail to replicate critical aspects of the corrosive environment, and consequently under- or over-estimate the real rate of corrosion in-service. One unique aspect of this particular program is the strong linkage between field and laboratory tests [4,5]. The salt deposits chosen for the laboratory tests were meant to mimic the real deposits collected from the one recovery boiler and two power boilers involved in the program. The equivalent field tests, in this case, typically ran for about 2000 h. As anticipated, exposure of the *in situ* coupons spanned a wide range of temperatures along the length of the probe, as well as very cyclic temperatures at each coupon location [4].

Overall, the general trends between field and laboratory trials matched well in the case of the *in situ* recovery boiler trials. N07214 (alloy F), N08028 (alloy C), and S31009 (alloy B) all performed poorly in the field. These alloys were also among the worst performers in the laboratory trials, particularly the N07214 (alloy F) at higher temperatures. The alloys that performed best in the *in situ* probes were N12160 (alloy I) and S21500 (alloy A), both of which also fared reasonably well in the laboratory tests. Although N06025 (alloy E) was clearly the best alloy in the laboratory tests, it did not fare as well at the higher temperatures in the field probe.

The correlations between laboratory and field results were less clear for the power boilers, because of the temperature differences [4]. The laboratory trials were conducted at significantly higher temperatures than could be reached in the locations where the field probes were installed, and consequently, there is no directly comparable data. In the case of the PB1 tests (Port Mellon boiler in the field trials), the maximum exposure temperature did not exceed 480°C in the field probe. Overall, the conditions in this boiler were much less corrosive than was the case in the PB2 boiler (Crofton). This matches the laboratory experience. However, an interesting note is that the most rapid corrosion in the field trial in the

Port Mellon boiler occurred at temperatures between 400°C and 450°C. This was attributed to the presence of Zn and Pb in the deposits, which form low-melting eutectic compounds at those temperatures. This is a good example of not replicating the critical corrosive environment in a laboratory test. These elements were not included in the synthetic salts due to their low concentrations in mill deposit samples (<0.2 wt%), nor was the test temperature in the appropriate range for this corrosion mechanism.

For the PB2 boiler, the maximum exposure temperature in the field was about 550°C. The best performing alloys in the field were N08120 (alloy D) and S21500 (alloy A), neither of which did particularly well at the higher temperature laboratory tests. N06025 (alloy E) was also not a good performing alloy in the field trials, despite doing well in the laboratory tests.

Across all three boilers, corrosion in the field trials was roughly of the same order of magnitude, but somewhat higher than those measured in the laboratory experiments. This is a good correlation, given the longer exposure times in the field trials. Cyclic temperatures and heat flux are also known to be strong accelerators for corrosion in high temperature conditions, and neither of these was present in the laboratory experiments. The difference in corrosion behavior for N06025 (alloy E) between the laboratory and field trials was surprising and merits further investigation, given the good performance of this alloy in the laboratory.

Implications for existing boilers

While the objective of the research program was to explore materials options for advanced biomass-fired boilers operating under extreme process conditions, some findings and observations from the laboratory test program can be applied directly to existing boilers. In general, the results from this test program compare reasonably with other studies of corrosion of superheater alloys in wood-fired and chemical recovery boilers [8-10]. Although not all of the alloys used in this project are currently available as code-certified materials for use as boiler tubes, the results suggest some might serve well under more realistic operating conditions (surface temperatures < 525°C) in kraft recovery boilers. However, caution is required in extrapolating these test results to long-term performance in a boiler. A corrosion rate of 0.22 mm/year or less was arbitrarily chosen as acceptable for the purposes of these tests; such a rate of corrosion might still be too high for practical application in a boiler. One consideration touched upon in another part of this program is whether the financial gain from producing more steam (and hence more electricity) could offset the cost of more frequent repairs/replacement of superheater elements due to increased corrosion from hotter, more challenging, environmental conditions [3].

Measured corrosion rates in the laboratory tests conducted below the FMT of the deposits were low, and the corresponding *in situ* probe results show relatively low corrosion rates, particularly for N06025 and S21500 [3,4]. Overall, N06025 did relatively well in laboratory tests. The laboratory data was not so positive for S21500, but for its alloy content, it did very well compared to alloys with much greater nickel and chromium content. The baseline alloys used for these studies (S31009 and S34709) are occasionally selected for use in higher temperature steam loops in recovery boiler superheaters [1], so alloys in this program that performed the same as or better than S31009 should do equally well in similar service.

On the hog fuel-fired boiler side, corrosion rates were significantly greater for all alloys in the salts representative of a highly chloride-contaminated fuel. In the more benign fuel, corrosion rates of all of the tested alloys were quite low. These results were mirrored by the *in situ* probes [3]. One interesting observation is that corrosion in the power boiler environments was driven strongly by direct contact with the deposits. This information could be valuable for mills that employ risk-based inspection protocols.

SUMMARY AND CONCLUSIONS

- A laboratory test was developed that allows for assessment and comparison of corrosion that occurs above and below deposits on the same coupon in simulated fireside superheater environments.
- In these tests, the rate of corrosion in the gas phase of simulated power boiler environments was substantially lower than for corrosion that occurred underneath deposits. This observation may have strong practical implications for companies that practice risk-based inspection in biomass-fired boilers.
- Under the test conditions employed, the vapor phase in the simulated kraft recovery boiler environment was found to be as aggressive to the alloys as the environment underneath salt deposits.
- In terms of best corrosion resistance, Alloy N06025 was ranked either first or second out of all the alloys evaluated in all laboratory test environments. The order of ranking of other alloys depended on the test environment, whether the corrosion was measured above or underneath the synthetic salt, and temperature.
- In an environment simulating a chloride-contaminated biomass-fired boiler, the alloy ranking at 650°C from most corrosion resistant to least is listed left to right below. (Roughly equivalent performance alloys are ranked together):

			R20033		
			N07214 (pre-oxidized)		
	N06025		N12160		N08120
Above salts:	N06025 (pre-oxidized)	<	S33228	<	S21500
	N06059		N07214		S31009
			N06690		
			N08028		

					N08120
					N12160
	N06025		N06059		S21500
Below salts:	N06025 (pre-oxidized)	<	N0714	<	N08028
	N06059 (pre-oxidized)		N06690		S31009
					S33228
					R20033

- In an environment simulating a kraft recovery boiler, the alloy ranking at 530°C from most corrosion resistant to least is listed left to right below (roughly equivalent performance alloys are ranked together):

			N12160		N08028
	N06059		N07214 (pre-oxidized)		S33228
Above salts (no SO_2):	N07214	<	N06690	<	S21500
	N06025		N08120		S31009
	N06025 (pre-oxidized)		R20033		

					N12160
Above salts (with SO_2):	N06690 N06025	<	N08120	<	S33228
					S21500
					S31009

			N12160		N07214 (pre-oxidized)
	N06059		N07214		N08028
Below salts (no SO_2):	N06025		S21500		S31009
	N06025 (pre-oxidized)	<	N06690	<	S33228
			R20033		
			N08120		

					N12160
Below salts (with SO_2):	N06025	<	N06690 N08120	<	S21500
					S33228
					S31009

- In an environment simulating a kraft recovery boiler with 625°C superheater tube temperature, all alloys were ranked as providing unacceptable performance. Based on these results, it is unlikely that a recovery boiler could be designed to operate at such a high temperature in the superheater. The alloy ranking at 625°C from most corrosion resistant to least was (left to right, roughly equivalent performance alloys ranked together):

			N12160		
	N06025		N06690		N06059
Above salts: (no SO_2)	N06025 (pre-oxidized)		N08120		N07214
	S21500	<	S33228	<	N07214 (pre-oxidized)
			S31009		
			N08028		
			R20033		

	N06025		N12160		S21500
Above salts (with SO_2):	N06025 (pre-oxidized)		N06690		
	N06059 (pre-oxidized)	<	N08120	<	
			S31009		
			S33228		

			S08120		
	N06025 (pre-oxidized)		N12160		N06059
Below salts: (no SO_2)	N06025		S31009		N07214
	N06690	<	S33228	<	N07214 (pre-oxidized)
	S21500		N08028		
			R20033		

					S31009
					N08120
Below salts (with SO_2):	N06025	<	N06690	<	S33228
					N12160
					S21500

ACKNOWLEDGMENTS

Jan van Heiningen, Greig Hull, Aleksey Bykov, Peggy Hung, Shannon Hoekstra, and Jonas Ritter are acknowledged for their contributions to specimen preparation, metallography, and analysis. Material for the corrosion samples was donated by Haynes International and Rolled Alloys. Funding was provided in support of this research by the member companies of FPInnovations, with support from the U.S. Department of Energy, Office of Energy Efficiency and Renewable Energy, Advanced Manufacturing Office under contract DE-AC05-00OR22725 with UT-Battelle, LLC, administered by James R. Keiser at the Oak Ridge National Laboratory and supported by in-kind contributions from the following project partners:

Åbo Akademi University, Andritz Oy, Babcock & Wilcox, Catalyst Paper, Chalmers University of Technology, Domtar Corporation, FM Global, FPInnovations, Foster Wheeler, Georgia Institute of Technology, Haynes International, Howe Sound Pulp & Paper, International Paper, MeadWestvaco, Metso Power, Outokumpu Stainless, Rolled Alloys, Sandvik Materials Technology, SharpConsultant, Southern Company, Special Metals, ThyssenKrupp VDM, University of Toronto Pulp and Paper Center, Vattenfall Power, and the Weyerhaeuser Company. **TJ**

LITERATURE CITED

1. Sharp, W.B.A., Singbeil, D.L., and Keiser, J.R., "Superheater corrosion produced by biomass fuels," *CORROSION/2012 Conf.*, NACE International, Houston, 2012, Product No. 51312-01308-SG.
2. Sharp, W.B.A, Singbeil, D.L, and Keiser, J.R., "Energy from biomass – Lessons from European boilers," *TAPPI PEERS Conf.*, TAPPI PRESS, Atlanta, GA, USA, 2011.
3. Sharp, W.B.A., Frederick, W.J., Keiser, J.R., et al., *TAPPI J.* 13(8): 65(2014).
4. Keiser, J.R., Sharp, W.B.A., and Singbeil, D.L., *TAPPI J.* 13(8): 51(2014).
5. Keiser, J.R., Sharp, W.B.A., Singbeil, D.L., et al., *TAPPI J.* 12(7): 45(2013).
6. Singbeil, D.L. and Frederick, L., "Improving heat recovery in biomass-fired boilers – Corrosion of superheater tube materials for high temperature black liquor and bark-fired boilers," Final Report ORNL Subcontract 4000089243, December 2012.
7. Mo-S System, "Bulletin of Alloy Phase Diagrams, Vol. 1, #2," American Society of Metals, Metals Park, OH, USA, 1980.
8. Tuiremo, J. and Salmenoja, K., "Control of superheater corrosion in black liquor recovery boilers," *Proc. - Int. Symp. Corros. Pulp Pap. Ind., 10th*, VTT, Espoo, Finland, 2001, Vol. 1, p. 181.
9. Mäkipää, M., Kauppinen, E., Lind, T., et al., "Superheater tube corrosion in recovery boilers," *Proc. - Int. Symp. Corros. Pulp Pap. Ind., 10th*, VTT, Espoo, Finland, 2001, Vol. 1, p. 157.
10. Salmenoja, K. and Mäkela, K., "Prevention of superheater corrosion in the combustion of biofuels," *CORROSION/2000 Conf.*, NACE International, Houston, 2000, Paper No. 00238.

ABOUT THE AUTHORS


Singbeil


Frederick


Keiser


Sharp

Pulp and paper mills have the potential to contribute significant amounts of electricity to North American power grids. However, corrosion of superheater tubes in our biomass and chemical recovery boilers limits their efficiency relative to coal-fired boilers. We wanted to find alloys that would perform well under extreme conditions – at superheater tube surface temperatures typical of coal-fired boilers. Identifying better materials for these tubes would increase the amount of steam available for conversion into electrical energy.

Our previous research has focused primarily on corrosion of water wall tubes in recovery boilers. A unique aspect of this work was the collaboration and breadth of the research program, including the supporting field trials conducted by Oak Ridge National Laboratory and economic evaluations by SharpConsultants reported in other papers of the same series [3,4].

Characterizing high temperature corrosion of small alloy samples in a meaningful way is extremely difficult in a laboratory setting. We used a statistical approach to measure damage and looked at effects of corrosion in the gas phase, under solid deposits, and in the presence of a melt – all in the same experiment. We found a few alloys that proved surprisingly resistant to corrosion in these environments, given their alloy content.

The test conditions used in these experiments were extreme for most existing boilers, but we found a few relatively cheap alloys that performed adequately and that would likely do very well in less extreme conditions. The next step in this research is another round of testing with less expensive alloys to identify best replacement superheater alloys for existing boilers that are looking for smaller gains in energy efficiency.

Singbeil is principal scientist and Frederick is principal technologist with FPInnovations, Vancouver, BC, Canada. Keiser is distinguished research and development staff member, Materials Science and Technology Div., at Oak Ridge National Laboratory, Oak Ridge, TN, USA. Sharp is principal at SharpConsultant in Columbia, MD, USA. Email Singbeil at douglas.singbeil@fpinnovations.ca.